Comparison of Dental Measurement Systems for Taxonomic Assignment of First Molars

Stefano Benazzi,[1,2]* Michael Coquerelle,[1] Luca Fiorenza,[2] Fred Bookstein,[1,3] Stanislav Katina,[4,5] and Ottmar Kullmer[2]

[1]*Department of Anthropology, University of Vienna, Vienna 1090, Austria*
[2]*Department of Palaeoanthropology and Messel Research, Senckenberg Research Institute, Frankfurt am Main D-60325, Germany*
[3]*Department of Statistics, University of Washington, Seattle, WA 98195*
[4]*Department of Applied Mathematics and Statistics, Comenius University, Bratislava 842 48, Slovakia*
[5]*Department of Statistics, University of Glasgow, Glasgow, Scotland G12 8QQ, United Kingdom*

KEY WORDS teeth; morphometrics; cervical outline; crown outline; Neanderthal

ABSTRACT Morphometrics of the molar crown is based traditionally on diameter measurements but is nowadays more often based on 2D image analysis of crown outlines. An alternative approach involves measurements at the level of the cervical line. We compare the information content of the two options in a three-dimensional (3D) digital sample of lower and upper first molars (M_1 and M^1) of modern human and Neanderthal teeth. The cervical outline for each tooth was created by digitizing the cervical line and then sectioning the tooth with a best fit plane. The crown outline was projected onto this same plane. The curves were analyzed by direct extraction of diameters, diagonals, and area and also by principal component analysis either of the residuals obtained by regressing out these measurements from the radii (shape information) or directly by the radii (size and shape information). For M^1, the crown and cervical outline radii allow us to discriminate between Neanderthals and modern humans with 90% and 95% accuracy, respectively. Fairly good discrimination between the groups (80–82.5%) was also obtained using cervical measurements. With respect to M_1, general overlap of the two groups was obtained by both crown and cervical measurements; however, the two taxa were differentiable by crown outline residuals (90–97%). Accordingly, while crown diameters or crown radii should be used for taxonomic analysis of unworn or slightly worn M^1s, the crown outline, after regressing out size information, could be promising for taxonomic assignment of lower M1s. Am J Phys Anthropol 144:342–354, 2011. ©2010 Wiley-Liss, Inc.

Traditional approaches for studying dental remains are characterized by morphological descriptions and caliper measurements of tooth crowns. Recent contributions in anthropology (e.g. Işcan and Kedici, 2003; Harris and Lease, 2005; Matsumura and Hudson, 2005) and paleoanthropology (e.g., Coppa et al., 2005; Bailey and Hublin, 2006; Kaifu et al., 2007) confirm that carefully prescribed caliper measurements (e.g., the mesiodistal diameter (MD) and the buccolingual diameter (BL)) remain useful tools for taxonomic studies.

Beginning in the 1960s, in keeping with the general turn to medical image analysis in many branches of the organismal biosciences, there were experiments with extraction of similar information from image analysis of occlusal surfaces (Hanihara, 1961; Erdbrink, 1965; Biggerstaff, 1970; Hanihara et al., 1970). These data include simple measurements such as area (Le Blanc and Black, 1974; Williams, 1979), quantifications of crown outline shape, configurations of landmarks from these images, and cusp base areas (Wood and Abbott, 1983; Wood et al., 1983; Morris, 1986; Sekikawa et al., 1988; Wood, 1991; Peretz et al., 1997, 1998a,b; Bailey, 2004; Bailey and Lynch, 2005; Harris and Dinh, 2006; Kondo and Townsend, 2006; Martinón-Torres et al., 2006; Peretz et al., 2006; Gómez-Robles et al., 2007).

It is obvious that all measurements of such occlusal surface images are affected by wear. This effect is not a problem when wear per se is the biological process of interest. However, in other study designs, wear is a confounding factor, altering not only crown height and cusp morphology but also crown walls and hence crown diameter data (Hillson et al., 2005). Accordingly, as Bailey (2004) and Bailey et al. (2005) concede, measurements taken at the cusp apices, such as cusp angles and occlusal polygon area, should be taken only from unworn or slightly worn teeth. Regarding the form of the outline in occlusal view, one approach would be to "correct" the corresponding measurements of mesial and distal crown margins by reference to the buccolingual extent of the wear facet along with the curvature of the crown margins in occlusal view (Wood and Abbott, 1983; Bailey, 2004; Bailey and Lynch, 2005). Many researchers recommend simply excluding heavily worn teeth from their

Grant sponsor: EU Marie Curie Training Network; Grant numbers: MRTN-CT-2005-019564 EVAN, VEGA 1/0077/09; Grant sponsor: NSF Hominid Grant 2007; Grant number: NSF 01-120.

*Correspondence to: Stefano Benazzi, Department of Anthropology, University of Vienna, Althanstraße 14, 1090 Vienna, Austria. E-mail: stefano.benazzi@univie.ac.at

Received 24 May 2010; accepted 26 August 2010

DOI 10.1002/ajpa.21409
Published online 10 November 2010 in Wiley Online Library (wileyonlinelibrary.com).

TABLE 1. List of fossil teeth[a] and 3D scan system used

Group	Lower M1	Scan systems	Upper M1	Scan systems
H. Neandertalensis	BDJ4C9 (l)[b]	microCT (NESPOS[c])	Combe Grenal (r)	Picza PIX-30
	Devils Tower (r)	Picza PIX-30	Krapina 100 (l)	smartSCAN 3D
	Krapina 80 (r)	Picza PIX-30	Krapina 134 (r)	Picza PIX-30
	Krapina 81 (l)	Picza PIX-30	Krapina 136 (l)	Picza PIX-30
	Krapina 84 (r)	smartSCAN 3D	Krapina 164 (l)	Picza PIX-30
	La Chaise 13 (l)	microCT (NESPOS)	Krapina 166 (r)	Picza PIX-31
	La Chaise 14 (r)	microCT (NESPOS)	Krapina 171 (r)	Picza PIX-30
	La Chaise S49 (r)	microCT (NESPOS)	Kulna 1 (r)	smartSCAN 3D
	La Quina 5 (r)	smartSCAN 3D	La Quina 18 (r)	smartSCAN 3D
	Okladnikov (l)	smartSCAN 3D	Pontnewydd 4 (r)	smartSCAN 3D
	Rochelet (l)	microCT (NESPOS)	Pontnewydd 12 (l)	smartSCAN 3D
	Regourdou 1 (r)	smartSCAN 3D	Spy 2 (l)	Picza PIX-30
	Petit Puy 3 (r)	Picza PIX-30	Poggio Cave (l)	Picza PIX-30
	Vindija 226 (l)	Picza PIX-30		
	Vindija 231 (l)	smartSCAN 3D		
UPMH[d]	Les Rois R50-4 (r)	Picza PIX-30	Fontéchevade 2 (l)	Picza PIX-30
	Sunghir 3 (r)	smartSCAN 3D	Sunghir 3 (l)	smartSCAN 3D
Modern humans	Medieval Italian ($n = 15$)[e]	Picza PIX-30	Medieval Italian ($n = 15$)[e]	Picza PIX-30
	Southern Asia ($n = 4$)[f]	smartSCAN 3D	Europe ($n = 4$)[g]	microCT
	Australian ($n = 3$)[g]	microCT	Australian ($n = 6$)[g]	microCT

[a] r, right; l, left.
[b] Name of the site: Abri Bourgeois-Delaunay "La Chaise-de-Vouthon."
[c] NESPOS Database/www.nespos.org.
[d] UPMH, upper Paleolithic modern human.
[e] Department of History and Methods for the Conservation of Cultural Heritage, University of Bologna (Ravenna, Italy).
[f] Department of Paleoanthropology and Messel Research, Senckenberg Research Institute (Frankfurt am Main, Germany).
[g] Department of Anthropology, University of Vienna (Vienna, Austria).

image analysis studies (e.g., Wood and Abbott, 1983; Kondo and Townsend, 2006; Martinón-Torres et al., 2006; Pilbrow, 2006; Gómez-Robles et al., 2007). However, such a strategy is disadvantageous for studies of paleoanthropological tooth assemblages, where sample size is very low already and dental remains are often significantly worn.

To incorporate worn teeth from archaeological or paleontological sites, Hillson et al. (2005) sought measurements less sensitive to enamel wear. They verified that cervical diameters and diagonals were correlated with the more usual crown measurements (Hillson et al., 2005) and hence might be a useful supplement for dental analysis in modern human samples. However, the reliability of these measurements for taxonomic assignment has not thus far been verified.

The present contribution evaluates the utility of information from diameters, diagonals, and outlines of two distinct closed curves (crown outline and cervical outline) for taxonomic assignment of Neanderthal and modern human isolated first molars.

MATERIALS

Our sample consists of 79 lower and upper M^1s, 47 from modern humans ($M_1 = 22$, $M^1 = 25$) and 32 that are casts of human fossil specimens ($M_1 = 17$, $M^1 = 15$) (Table 1). The modern sample includes Northern Italian medieval first molars and also specimens collected from the Department of Anthropology, University of Vienna, Austria and from the Department of Paleoanthropology and Messel Research in the Senckenberg Research Institute, Frankfurt am Main, Germany. The fossil material is represented mainly by Neanderthal specimens and Upper Palaeolithic modern humans (UPMH). For statistical analysis, the few UPMH specimens are combined with the contemporary *Homo sapiens*, but they are plotted with distinct labels. To avoid enamel reflection and transparency, as well as to prevent damage to the fossil originals, casts carefully reproduced by standard methods, as described elsewhere (Fiorenza et al., 2009), were used for three-dimensional (3D) surface scanning. In addition, some virtual tooth models were downloaded from the NESPOS (Neanderthal Studies Professional Online Service) digital internet archive (www.nespos.org) (Table 1).

Following the work of Bailey (2004) and the suggestions provided by Hillson et al. (2005) about measurements in worn molars, only first molars characterized by a slight or moderate degree of wear were considered (wear stage lower than 5; Smith, 1984).

All molars are regarded as left molars—actual right molars were mirror-imaged prior to any further computations.

METHODS

All the teeth from the Italian medieval sample and some casts from the fossil specimens were scanned with a Roland Picza PIX-30 piezoelectric digitizer provided with a Roland Active Piezo Sensor (R.A.P.S.) probe with a resolution of 0.1 mm (Table 1). The 3D model of each tooth was generated with Pixform 2001 software. Microcomputer tomography models (micro-CT) of molars from the Vienna anthropological collection were acquired using Viscom X8060. All micro-CT scans were recorded in TIFF file format (pixel size 70 μm, slice thickness also 70 μm). The 3D digital models were built via the software package Amira 5.2 (©Mercury Computer Systems, Chelmsford, MA). Models were created semi-automatically by threshold-based segmentation, contour extraction, and surface reconstruction. Other casts were scanned using a smartScan 3D system (Breuckmann GmbH), with a resolution of about 60 μm (Breuckmann, 1993; Beraldin et al., 2000; Godin et al., 2002). The final

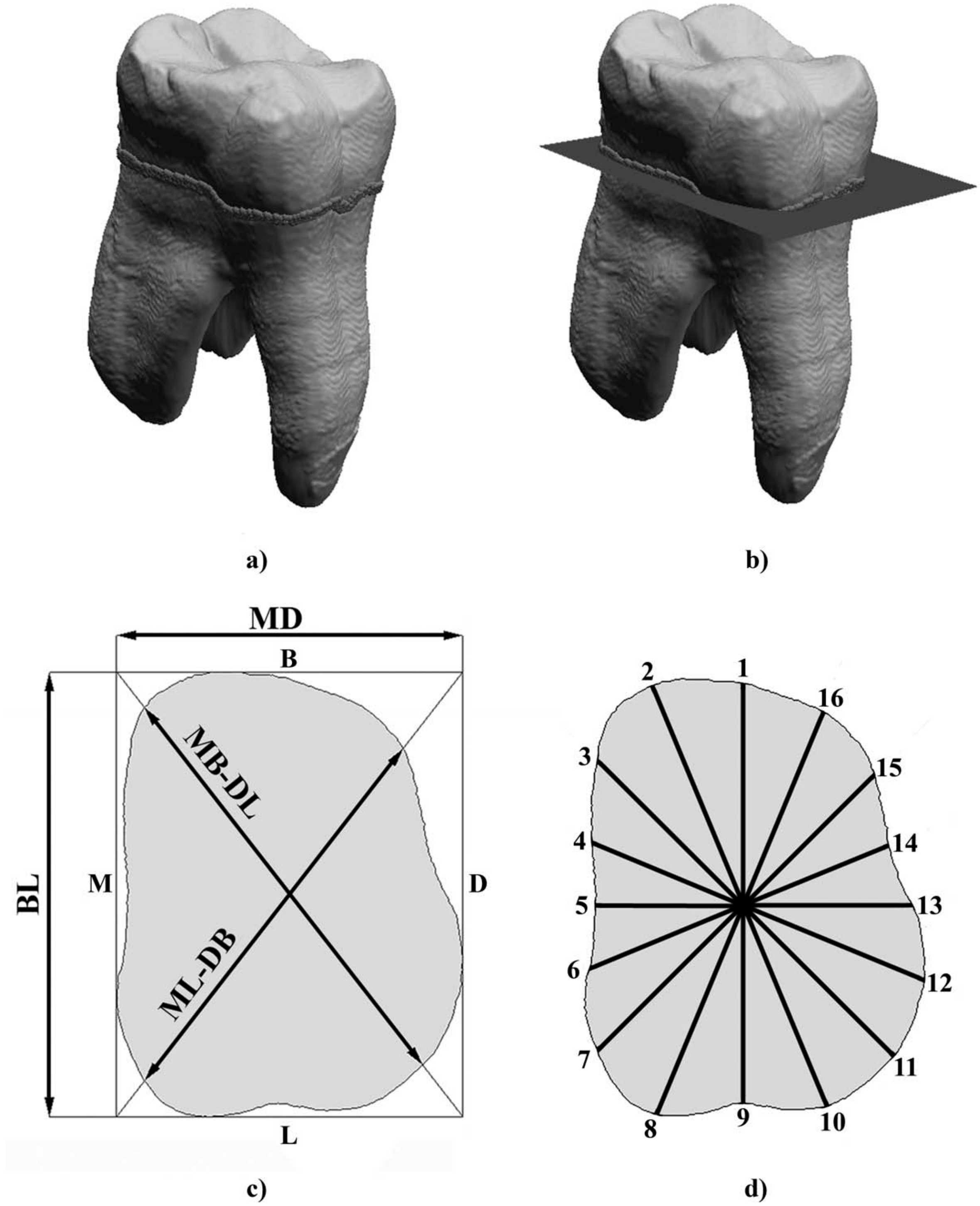

Fig. 1. Upper left first molar. (**a**) Triangle vertices were selected up to a maximum distance of 0.2 mm above and below the cervical polyline. (**b**) Best-fit plane passing through the triangle vertices. (**c**) Bounding box of the cervical outline with displayed diameters and diagonal measurements. (**d**) 16 equiangular radii out of the centroid of the area. The first radii is buccally directed and parallel to the *y*-axis of the Cartesian coordinate system.

alignment of the views was achieved using optoCAT software 2007 (Breuckmann GmbH).

The 3D digital tooth models were preoriented in Rhino 4.0 Beta CAD environment (Robert McNeel & Associates, Seattle, WA), according to the description given by Benazzi et al. (2009), to define buccal, lingual, mesial, and distal views of the tooth. The models were positioned with the occlusal view parallel to the *xy*-plane of the Cartesian coordinate system. On the buccal and lingual side of the molars, two points were identified at the intersection of the cervical line with the line joining the most cervical point of the bifurcation of the root and the most apical point of the groove dividing the two main lobes of each surface. The tooth was rotated until the projection on the xy-plane of the segment joining the two points was parallel to the y-axis of the Cartesian coordinate system (Benazzi et al., 2009).

In the IMEdit module of PolyWorks® 10 (InnovMetric Software), the cervical lines of the preoriented teeth were manually outlined using the polyline tool and all surface model triangle vertices were selected that lay within 0.2 mm of the cervical polyline (Fig. 1a). This method compensates for model and processor errors (Kullmer et al., 2002; Ulhaas et al., 2004) such as those that originate in cervix defects in the original crowns or otherwise. It also corrects for the minor mistakes in drawing the polyline where small portions of the cervical line are not visible in the digital model. Next, we computed the best-fit plane through the band of selected vertex points (cervical plane: Fig. 1b). This plane sections the tooth in a curve that we take as the cervical outline. Maintaining the same preorientation, each tooth was subsequently rotated until the cervical plane was parallel to the xy-plane. The crown was projected onto this xy-plane and its outline (horizon) taken, a planar representation of what is in reality a nonplanar curve. Both crown outline and cervical outline were centered on the centroid of their area. Bounding boxes were displayed (Fig. 1c) tangential to the most extreme points of the crown and cervical sides (MD and BL diameters). The diagonals of the bounding boxes, mesiobuccal-distolingual (MB-DL) and mesiolingual-distobuccal (ML-DB), were taken as the diagonals of the teeth.

The diameters and diagonals measured on these outlines are not exactly the same as those conventionally measured by calipers. As pointed out by Hillson et al. (2005), small rotations of the crown between the caliper jaws can lead to variations in the measured diameter of 1 mm or more, and personal judgment is often involved in any attempt to keep the calipers in correct position (Hillson et al., 2005). Moreover, there are several alternative criteria for crown diameter measurements (e.g., Moorrees and Reed, 1954; Goose, 1963; Kieser, 1990), with different results depending on the method used. Our objective and replicable approach (Fig. 1) avoids these problems by representing the occlusal surface as a curve. Where teeth showed interproximal wear, the crown outline of the original mesial or distal borders were corrected by reference to the buccolingual extent of the wear facet, the outline curvature following the crown margins in occlusal view (e.g., Wood and Engleman, 1988; Bailey, 2004).

All outlines were represented by 16 equiangularly spaced radial vectors out of the centroid of area. The first radius is buccally directed and parallel to the y-axis (Fig. 1d). Outline size was computed as the root sum of squared radii (thus a radial equivalent of "centroid size"). The radii measure shape and size of the outlines and thus covary with diameters, diagonals, and area. Therefore, we regressed the part of radial size explained by diameters, diagonals, and area out of the actual crown and cervical outline data, to evaluate the possible usefulness of the residual shape variation for classification of Neanderthal and modern human teeth. That is to say, for both the crown outline and the cervical outline, we carried out linear regressions of the 16 radii, one by one, on both MD and BL, then on both MB-DL and ML-DB, and finally on the area. The "residual shape" is just the shape formed by the 16 residuals of these radii after these regressions; evidently, it does not correspond to a geometric figure (as about half of the radii will be negative case by case). As there were three families of regressions, diameters, diagonals, and area, there were three residual shapes for the crown outline and three for the cervical outline. For each of the two outlines, principal component analysis (PCA) was carried out both for the original radii and for the three sets of regression residuals: a total of eight PCAs for each tooth class.

TABLE 2. Lower M1 outline area (mm^2): mean and standard deviation (SD)

Groups	N	Crown outline area		Cervical outline area	
		Mean	SD	Mean	SD
Modern humans[a]	24	104.31	12.01	76.75	9.51
Neandertals	15	108.66	8.54	83.00	6.47

[a] UPMH is included.

Finally, the discriminant function analyses we use are quadratic discriminant analyses (QDAs) rather than the more commonly encountered linear discriminant analyses (LDAs). This is because for some of our measurements, particularly the outlines area in Table 4, the within-group variances are different between our two taxonomic groups. When the standard deviations are different and are acknowledged to be different, the corresponding log likelihood ratio is actually a quadratic function (a function of x^2 as well as x), hence we use a "quadratic" discrimination. A QDA is not the same thing as a LDA that uses x and x^2 as the predictors—this approach would not take into account the difference in standard deviations between the groups, which is the point of QDA. A QDA, for instance, can discriminate between two groups that have the same average if their variances are different enough—that is the situation in Tables 2 and 4—whereas a LDA cannot do so. The QDAs of the dental dimensions (diameters, diagonals, and area) and of a subset of principal components (PCs) were used to classify the specimens. We restricted ourselves to five principal components to accommodate a majority of the shape variability (usually about 80%) while avoiding overfitting. We use a cross-validation approach (a leave-one-out method) to assign the specimen to the group with the higher posterior probability. For data processing and analyses, we used software routines written in R software (R Development Core Team, 2008).

RESULTS

In general, the PC plots of the residuals from the regression of the diameters, diagonals, and area for the crown and cervical outline produce equivalent results regardless of the particular regression. Therefore, for each tooth class we display only four of the PCAs: two computed from crown and cervical outline residuals (M_1: residuals obtained after regressing out the diameters; M^1: residuals obtained after regressing out the area), and another two from the original radii. Here PC1 is always highly correlated with radial size ($r = 0.99$).

Lower M1

Figure 2 and Table 2 show that Neanderthals, UPMH and modern humans overlap to a large extent regarding diameters, diagonals, and areas measured either at the crown outline or at the cervical outline. The group averages of these measurements do not differ significantly between Neanderthals and modern humans

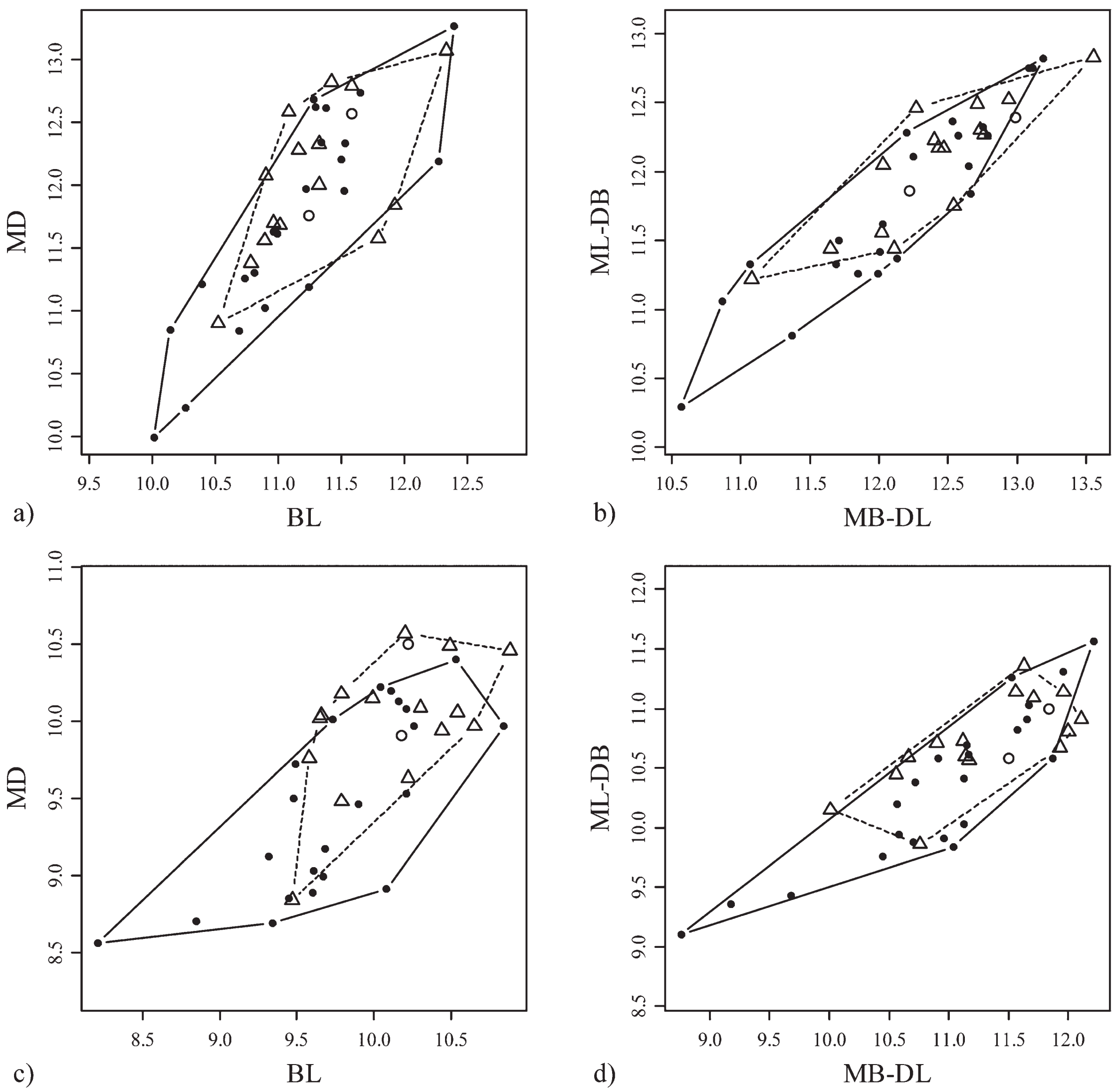

Fig. 2. Scatterplot of M_1 crown and cervical measurements. (**a**) BL and MD crown diameters. (**b**) MB-DL and ML-DB crown diagonals. (**c**) BL and MD cervical diameters. (**d**) MB-DL and ML-DB cervical diagonals. Modern humans, black circles; Neanderthals, triangles; UPMH, white circles.

(P-value $>$ 0.05 by permutation test, 1,000 permutations). The cross-validation QDA of these dimensions (diameters, diagonals, and areas) leads to a high misclassification of Neanderthals and modern humans (Table 3).

The results of the PCAs of the crown and cervical outlines are summarized in Figures 3 and 4. Regarding the crown residuals obtained after regressing out the crown diameters from the crown radii (Fig. 3a), the first three PCs account for 60.3% of the total variance. Neanderthals and modern humans tend to separate along PC1, while there is no such trend for PC2 or PC3. In the direction of PC1, Neanderthals show a buccodistal outline expansion and a convex lingual outline shape (high scores), while modern human and UPMH specimens are associated with a buccodistal reduction of the outline and a straighter lingual side (low scores). The results of the cross-validation QDA show that 94.9% of the Neanderthals and modern humans are correctly classified based on crown outline residuals (Table 3).

The PCA and cross-validation QDA of the crown radii do not provide better results than the crown outline residuals (Fig. 3b, Table 3). The first three PCs account for about 93.7% of the total variance. Neanderthals and modern humans overlap along PC1 and PC2, but they tend to separate along PC3. PC3 reflects shape changes related to buccodistal outline expansion and convex lingual outline shape (low scores: Neanderthal shape), and buccodistal reduction with straighter lingual side (high scores: modern human shape). The UPMH specimens plot with the modern humans (Fig. 3).

Regarding the cervical outline residuals (cervical diameters regressed out from the cervical radii, Fig. 4a), the separation between Neanderthals and modern humans—including UPMH specimens—is less clear than for the crown residuals. The two groups overlap along each of the first three PCs. The results of the cross-validation QDA shows that about 75% of Neanderthals and modern humans are correctly classified (Table 3). The results do not improve using the cervical radii (Fig. 4b, Table 3). While the first three PCs account for a large amount of the total variance (92.5%), there remains a large overlap in each direction. By cross-validation QDA,

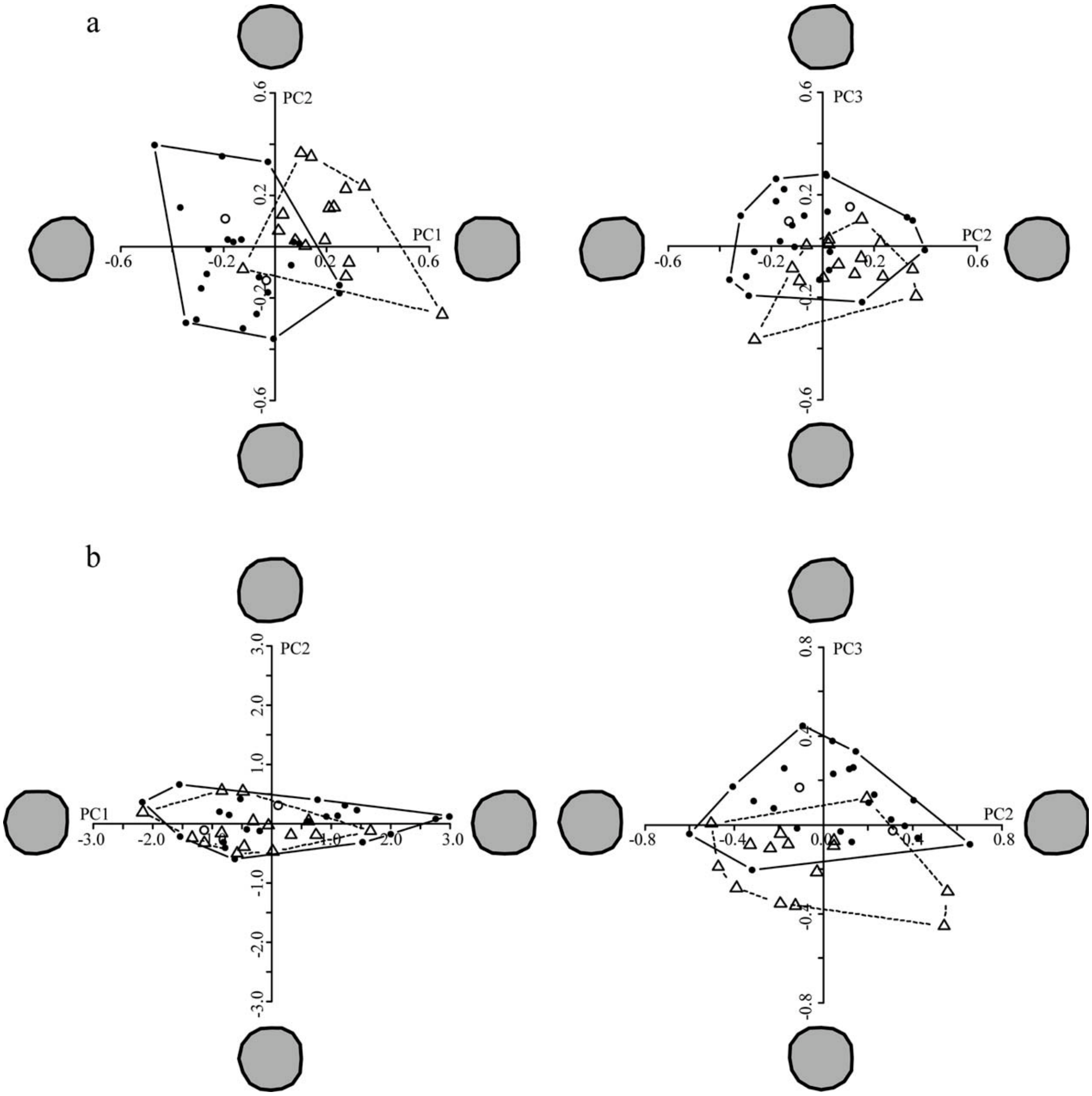

Fig. 3. M_1 crown outline. (**a**) PCA of the residuals after regressing out crown diameters from the crown radii. (**b**) PCA of the crown radii. At each extremity of the axes is drawn the deformed mean crown outline in the direction of the PC, extrapolated by a factor of 3SD of PCs. Modern humans, black circles; Neanderthals, triangles; UPMH, white circles.

61.5% of Neanderthals and modern humans are correctly classified (Table 3).

Upper M1

Unlike the case for M_1, for M^1, the diameters, diagonals and areas measured either at the crown outline or the cervical outline overlap to a much lesser extent between Neanderthals and modern humans (Fig. 5, Table 4). The group means of these dimensions are significantly different between Neanderthals and modern humans except ML-DB at the cervical outline. For crown and cervix, the few UPMH specimens plot between the middle-upper modern human range. The results of the cross-validation QDA show that the diameters, diagonals and areas allow correct classification of between 80% and 82.5% of the Neanderthals and modern humans (Table 5).

Figures 6 and 7 summarize the results of the PCA of the crown and cervical outlines. Figure 6a shows the PCA of the residuals obtained after regressing out areas from the crown radii. The first three PCs account for 76.6% of the total variance. The UPMH specimens plot within the modern human sample. Neanderthals and modern humans tend to separate on PC1 but not PC2 or PC3. Along PC1, Neanderthal specimens (higher scores) are associated with a wide distolingual outline as a result of a large hypocone, a slight expansion of the mesiobuccal side and a reduction of the distobuccal outline, while modern humans (lower scores) show a subsquare shape, with a narrow distolingual outline and a slight expansion of the distobuccal side. The cross-valida-

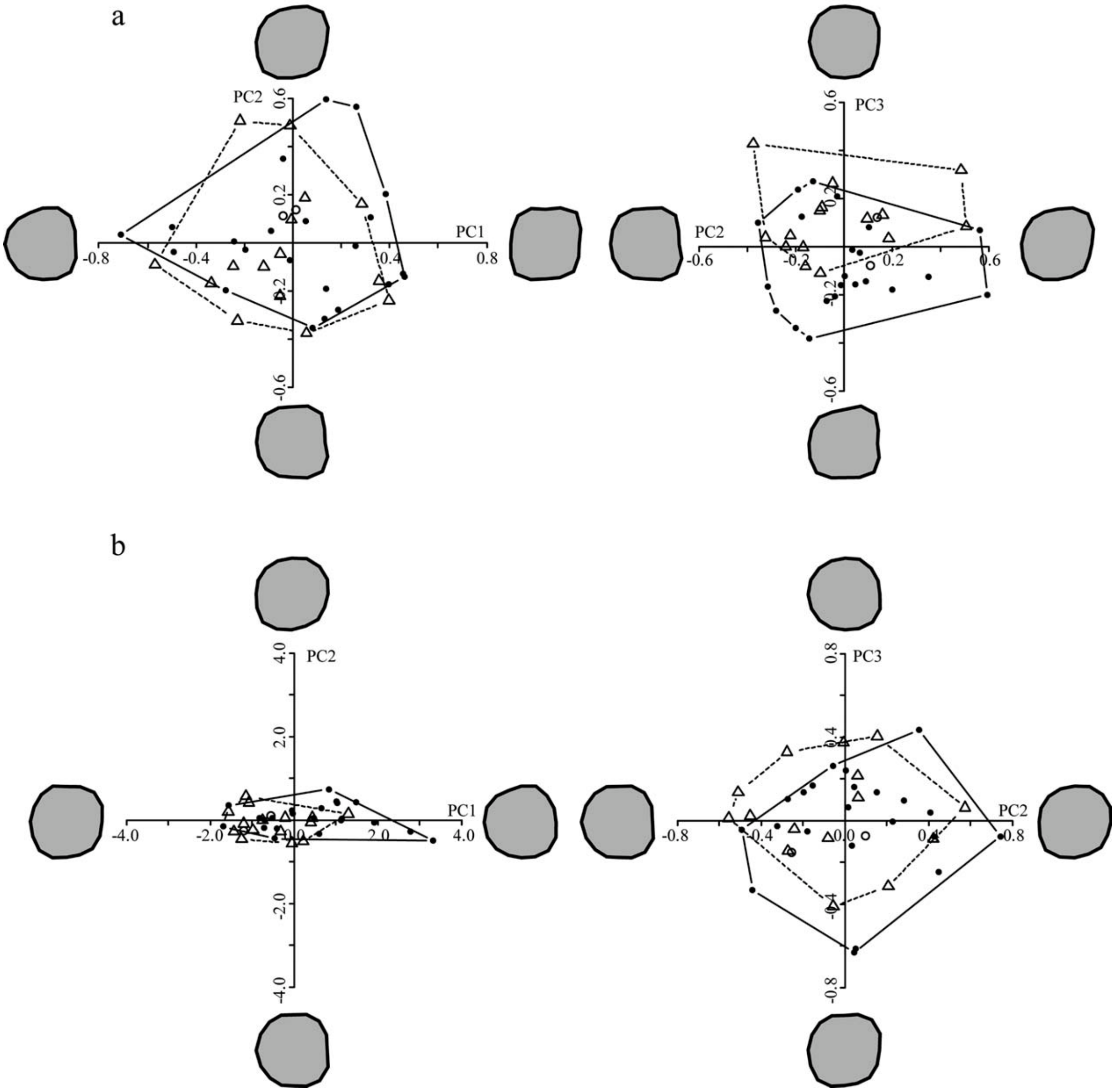

Fig. 4. M_1 cervical outline. (**a**) PCA of the residuals after regressing out cervical diameters from the cervical radii. (**b**) PCA of the cervical radii. At each extremity of the axes is drawn the deformed mean crown outline in the direction of the PC, extrapolated by a factor of 3SD of PCs. Modern humans, black circles; Neanderthals, triangles; UPMH, white circles.

tion QDA of the crown outline residuals leads to a correct classification of 85% of the specimens (Table 5). Figure 6b shows the PCA of the crown radii. The first three PCs account for 94% of the total variance. Neanderthals and modern humans are separated on PC1 which is, of course, correlated with size. Neanderthals show a wide distolingual outline (higher scores) and consequently an almost rhomboidal shape, while modern humans (lower scores) are characterized by a subcircular outline. To a lesser extent, the two groups seem to have different means on PC2, but not PC3 (Fig. 6b). Lower PC2 scores are associated with distolingual outline expansion (Neanderthal shape), while higher PC2 scores account for subcircular shape due to distobuccal and mesiolingual outline expansion and distolingual outline reduction (modern human shape). The UPMH specimens plot within the modern human sample. When the four PCs obtained for the crown radii are submitted to cross-validation QDA, 95% of the specimens are correctly classified (Table 5).

With respect to the cervical residuals (the cervical area regressed out from the cervical radii, Fig. 7a), the first three PCs account for about 82% of the total variance. Neanderthals and modern humans tend to have different means on PC1 but not PC2 and PC3. As for the crown, the cervical outline shows a distolingual expansion in Neanderthals (higher PC1 scores), while modern humans are characterized by mesiodistal outline compression with concomitant subrectangular shape and distolingual outline reduction (lower PC1 scores). The UPMH specimens provide variable results; Fontechevade-2 fits in the modern human sample while Sunghir-

TABLE 3. Results of QDA for the lower M1[a]

Dental measurements	Misclassified: Modern humans[b]	Misclassified: Neandertals	Total misclassified	Correctly classified (%)
Crown				
Diameters	4	13	17	56.4
Diagonals	5	14	19	51.3
Outline area	7	15	22	43.6
PCs[c] (diameter regressed)	1	1	2	94.9
PCs (diagonal regressed)	1	0	1	97.4
PCs (area regressed)	2	2	4	89.7
PCs (centered radii)	1	2	3	87.2
Cervical				
Diameters	10	7	17	56.4
Diagonals	8	10	18	53.8
Outline area	10	7	17	56.4
PCs (diameter regressed)	5	5	10	74.5
PCs (diagonal regressed)	4	7	11	71.8
PCs (area regressed)	3	9	12	69.2
PCs (centered radii)	6	9	15	61.5

[a] Results after cross-validation.
[b] UPMH is included.
[c] PCs, principal component scores (the first five PCs were used for QDA).

3 plots with the Neanderthals. The results of the cross-validation QDA show that 75% of the specimens are correctly classified.

The results improve using the cervical radii (Fig. 7b, Table 5). The first three PCs account for a large amount of the total variance (93%). The two groups are well separated in the direction of PC1. The shape change associated with PC1 also includes the distolingual expansion (higher scores) or reduction (lower scores) of the outline. Shape information related to the same portion of the outline is contained in PC2 but not in PC3. Neanderthals are characterized by a rhomboidal cervical outline due to distolingual expansion (lower PC2 scores), while modern humans show subsquare outline (higher PC2 scores). For PC1, the UPMH specimens plot in between Neanderthal and modern human, but Fontechevade-2 scores closer to modern humans with regard to PC2, while Sunghir-3 scores closer to Neanderthals on PC3 (Fig. 7b). When the first four PCs are submitted to cross-validation QDA, 90% of the Neanderthals and modern humans are correctly classified (Table 5).

TABLE 4. Upper M1 outline area (mm^2): mean and standard deviation (SD)

Groups	*N*	Crown outline area: Mean	Crown outline area: SD	Cervical outline area: Mean	Cervical outline area: SD
Modern humans[a]	27	108.90	8.21	82.70	6.75
Neandertals	13	124.97	19.41	98.08	13.31

[a] UPMH is included.

DISCUSSION AND CONCLUSIONS

It is important to know whether the more time-consuming measurements (such as outlines or areas) are worth the trouble for these taxonomic purposes, particularly in regard to circumventing the effects of wear. In unworn teeth, 2D image analysis of cusp area or the occlusal polygon might provide for adequate taxonomic assignment of isolated first molars. The challenge is to include worn teeth for which the cusp tips are obscured and the occlusal grooves may no longer be visible. In this condition, both the traditional approach based on caliper measurements at the crown (e.g., Işcan and Kedici, 2003; Coppa et al., 2005; Harris and Lease, 2005; Matsumura and Hudson, 2005; Bailey and Hublin, 2006; Kaifu et al., 2007) and the 2D image analysis of the occlusal surface (Wood and Abbott, 1983; Wood et al., 1983; Sekikawa et al., 1988; Wood, 1991; Peretz et al., 1997, 1998a,b; Bailey, 2004; Bailey and Lynch, 2005; Harris and Dinh, 2006; Kondo and Townsend, 2006; Peretz et al., 2006; Gómez-Robles et al., 2007) are limited by reduced sample sizes and the need to reconstruct missing outlines (Wood and Abbott, 1983; Wood et al., 1983). Moreover, since the maximum MD crown diameter of the molars is generally one-third to one-half of the way from the occlusal surface to the cervix, even modest interproximal wear can affect MD diameters (Hillson et al., 2005); but the maximum BL diameter, measured at one-third to one-half from the cervix, is not affected even in Smith wear stage 4 (Smith, 1984).

We find that, at least for the lower molar, a more thorough metric examination could lead to better discrimination between Neanderthals and modern humans, and that cervical measurements (diameters, diagonals, and area) could provide classification accuracy similar to those from crown measurements in upper M1s.

For M^1, diameters, diagonals and areas either at the crown or at the cervix are sufficient to classify our two taxa at up to 82.5% accuracy (Fig. 5, Table 5). Even after diameters, diagonals and areas are regressed out from the crown and cervical radii (Figs. 6 and 7), morphological peculiarities such as the well-known hypocone enlargement seen in Neanderthal maxillary first molars (e.g., Bailey, 2002, 2004; Gómez-Robles et al., 2007) are still present. Despite that, the percentage of Neanderthals and modern humans correctly classified does not improve (Table 5). The original crown and cervical radius values, in which both size and shape information are still present, leads to a better classification compared with diameters, diagonals and area—up to 95% accuracy. We suggest that crown diameters or crown radii should be used for taxonomic analysis of unworn or slightly worn M^1, and that for worn, isolated M^1, measurements

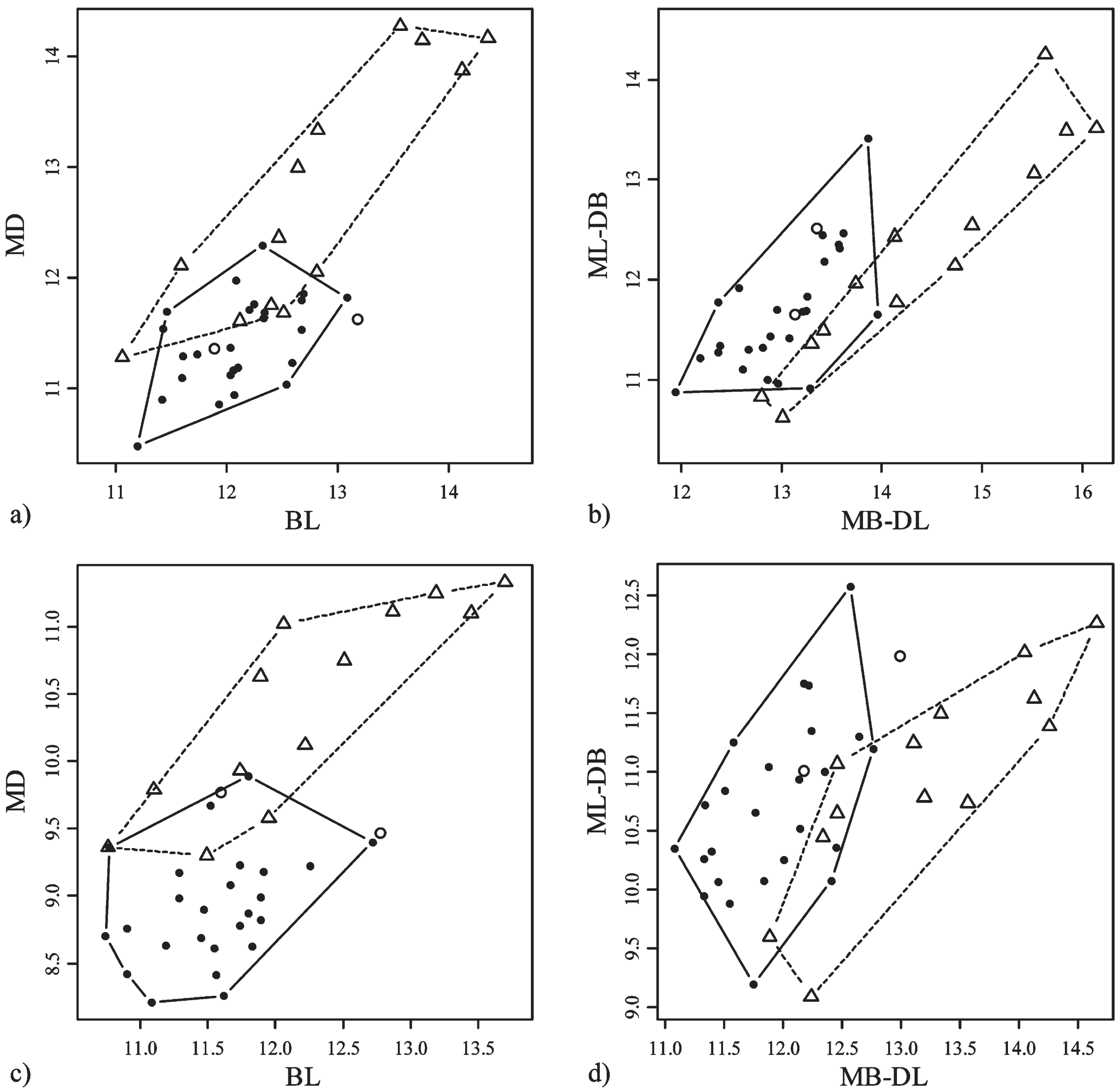

Fig. 5. Scatterplot of M^1 crown and cervical measurements. (**a**) BL and MD crown diameters. (**b**) MB-DL and ML-DB crown diagonals. (**c**) BL and MD cervical diameters. (**d**) MB-DL and ML-DB cervical diagonals. Modern humans, black circles; Neandertals, triangles; UPMH, white circles.

TABLE 5. Results of QDA for the upper M1[a]

Dental measurements	Misclassified: Modern humans[b]	Misclassified: Neandertals	Total misclassified	Correctly classified (%)
Crown				
Diameters	2	5	7	82.5
Diagonals	2	5	7	82.5
Outline area	1	7	8	80.0
PCs[c] (diameter regressed)	3	5	8	80.0
PCs (diagonal regressed)	3	5	8	80.0
PCs (area regressed)	0	5	5	87.5
PCs (centered radii)	0	2	2	95.0
Cervical				
Diameters	4	3	7	82.5
Diagonals	3	5	8	80.0
Outline area	2	6	8	80.0
PCs (diameter regressed)	7	12	19	52.5
PCs (diagonal regressed)	4	6	10	75.0
PCs (area regressed)	4	6	10	75.0
PCs (centered radii)	2	2	4	90.0

[a] Results after cross-validation.
[b] UPMH is included.
[c] PCs, principal component scores (the first five PCs were used for QDA).

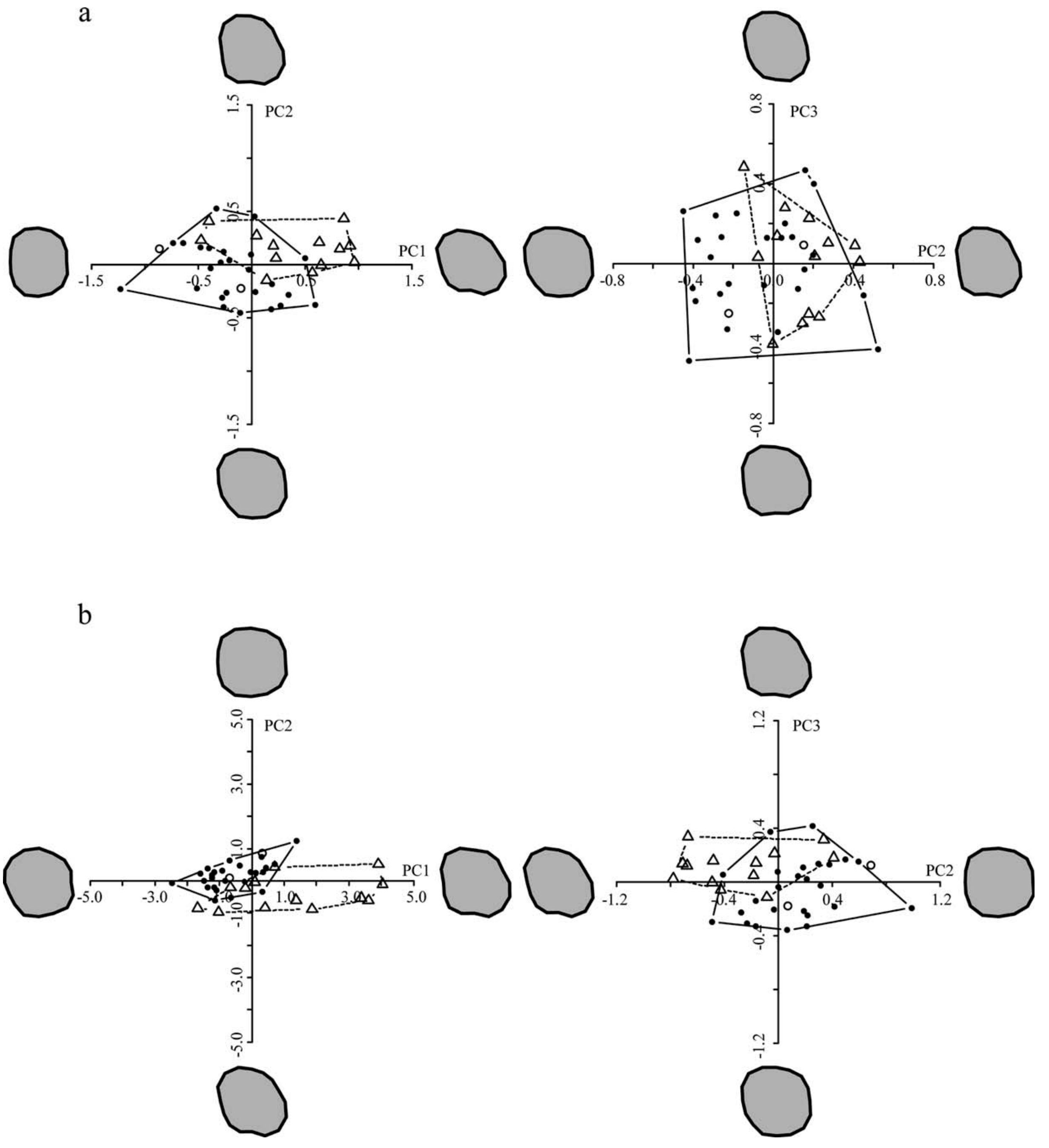

Fig. 6. M^1 crown outline. (**a**) PCA of the residuals after regressing out crown area from the crown radii. (**b**) PCA of the crown radii. At each extremity of the axes is drawn the deformed mean crown outline in the direction of the PC, extrapolated by a factor of 3SD of PCs. Modern humans, black circles; Neanderthals, triangles; UPMH, white circles.

at the cervix (diameters, diagonals, and area but also cervical outline radii) are a reliable alternative.

In contrast to the situation with M^1, for M_1 the crown and cervical diameters, diagonals and areas barely differentiate Neanderthals from modern humans at all (Fig. 2, Table 3). Once crown measurements are regressed out from the crown radii, the levels of classifications are considerably higher, ranging up to 97.4% (Table 3). In other words, while the grosser crown measurements are useless for distinguishing between Neanderthal and modern human M_1s, some morphological crown outline features account for interesting taxonomic differences between the two taxa: a reduction of the buccodistal outline (related to the hypoconulid) and the straighter lingual side in modern humans when compared to Neanderthal M_1s. Moreover, the classifications based on crown residuals and crown radii are more accurate than those based on cervical residuals and cervical radii.

Yet the most heavily worn M_1, those with only a few millimeters of the crown height preserved, can be classified only with difficulty. This is a general consideration that limits the results of any kind of surface analysis of the M_1 for the strictly taxonomic purpose exemplified

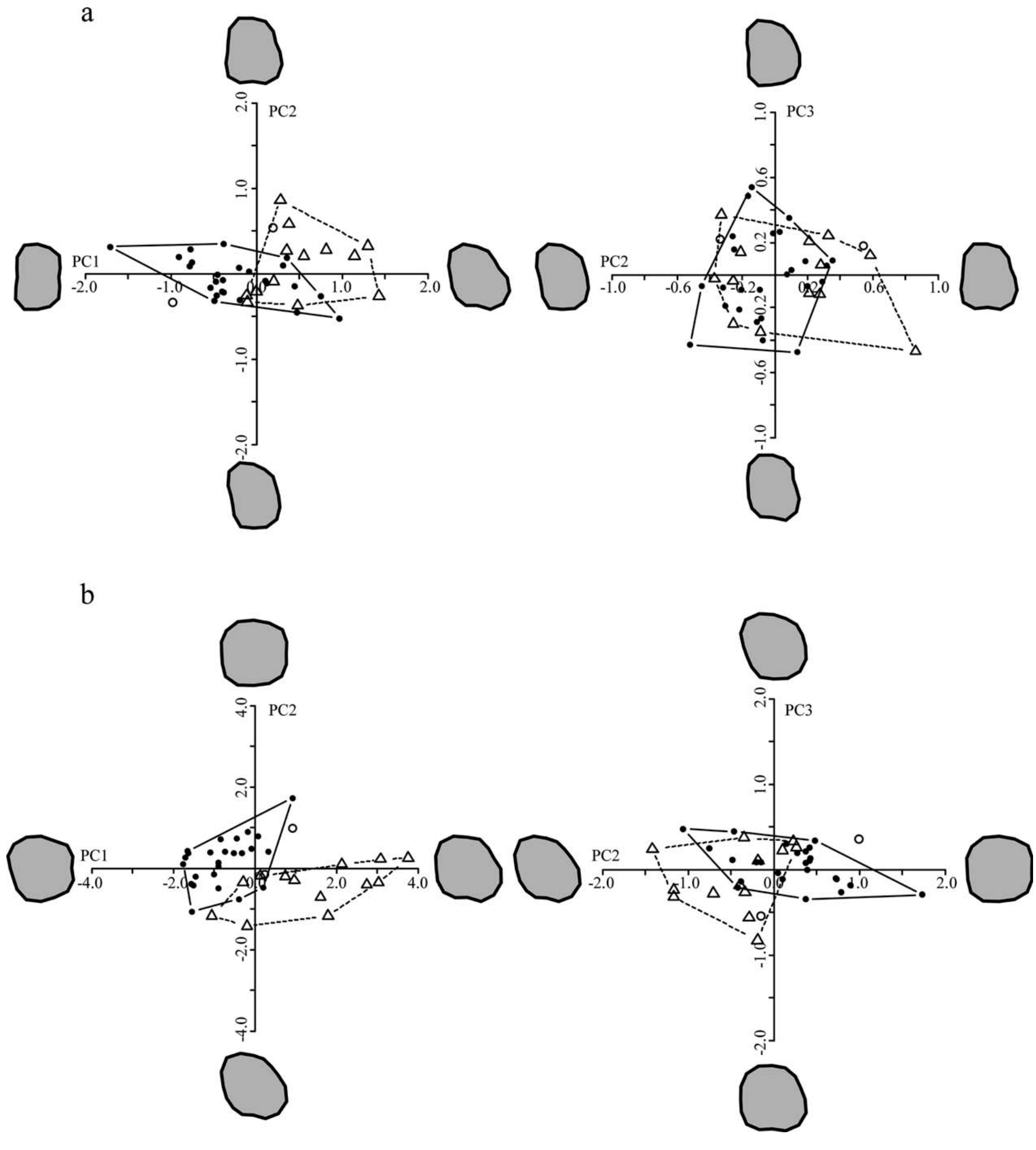

Fig. 7. M^1 cervical outline. (**a**) PCA of the residuals after regressing out cervical area from the cervical radii. (**b**) PCA of the cervical radii. At each extremity of the axes is drawn the deformed mean crown outline in the direction of the PC, extrapolated by a factor of 3SD of PCs. Modern humans, black circles; Neanderthals, triangles; UPMH, white circles.

here. In fact, if unworn or less worn M_1s are considered, nonmetric traits alone could underlie a reliable taxonomy (e.g., Bailey, 2002). Indeed, we have also shown that the crown outline, after regressing out size information, could be promising for taxonomic assignment of lower M1. Nevertheless, when M_1s are so heavily worn that large dentine basins are exposed, less information is preserved and traditional measurements at the cervical line fail to distinguish satisfactorily between Neanderthals and modern humans. Perhaps the information contained in the cervical residuals could supply a classification with accuracy in the 70–75% range.

If the cervical outline approach is to be as useful as we think it ought to be, we need a database of these hitherto unusual measurements. Since a 3D model of the tooth is required in order to mark the cervical line, the method is obviously more time-consuming than caliper-based methods. It should be used only where it promises real advantages. Moreover, the approach used here for orienting the teeth (based on the best-fit plane at the cervical line and the BL axis, see above) may not be the best solution for other tooth classes. Although the cervical line of the molars is almost flat, mesial and distal cervical lines in canines and incisors differ markedly between buccal and lingual sides. A best-fit plane section would provide an erroneous representation of the cervical line. Yet, an objective definition of the BL axis is required for tooth orientation. As mentioned earlier, MD and the BL diameters depend on the criteria for crown diameter measurements used (e.g., Moorrees and Reed, 1954; Goose, 1963; Kieser, 1990): the latter is usually measured perpendicular to the former and considered as the BL axis of the tooth (e.g., Hillson et al., 2005). This fact explains why we cannot rely on this subjectively defined BL axis for orienting teeth. Nevertheless, we also emphasize that the objective method shown here for identifying the BL axis (see above) would not be suitable in a maxillary molar with extremely reduced or not present hypocone. This last case, which affects the expression of the groove between protocone and hypocone, is not a serious problem when we only focus on M^1, but prevents an extension of the methodology to the second or third molars. Methods should be developed for each practical context.

Our results suggest that the association between shape and size is different for the upper and lower M1s and, importantly, in both teeth there is a species signature. Species information is carried by both size and size-independent shape for M^1, whereas species information is only revealed by size-independent shape for M_1. Accordingly, in both cases the size-independent shape of the crown outline holds important taxonomic information. How does the shape of the upper and lower M1 covary with respect to the species signal? On the basis of our sample, we could argue that the shape difference between Neanderthals and modern humans we observed at the distobuccal side of the lower M1, that is, the hypoconulid, is correlated to that which we observed at the distolingual side of the upper M1, that is, the hypocone. Nevertheless, to test this assumption, for instance via partial least squares analysis, and to examine the association between shape and size in both teeth, each paired upper and lower M1 must belong to the same individual. Such a study design is not possible using the Neanderthal fossil specimens currently available. Finally, despite our intention to create a representative fossil sample, we are aware that our sample cannot account for the whole variability of Neanderthal and UPMH upper and lower M1. Therefore, we emphasize that the results mentioned earlier are relevant for our fossil sample, but further work on the subject with a larger sample size is desirable.

ACKNOWLEDGMENTS

We thank Peter Ungar (Paleoanthropology Laboratory, University of Arkansas, Fayetteville, Arkansas, USA) for the use of the piezoelectric digitizer in his laboratory, Erik Trinkaus (Paleoanthropology Laboratory, Washington University, St. Louis, MO) for providing casts of Neanderthal and Upper Palaeolithic modern human teeth, and Gerhard Weber (Department of Anthropology, University of Vienna, Austria) and the Vienna micro-ct Lab for access to microCT data of first molars. We are grateful to the following curators and institutions for access to comparative and fossil specimens: Marta Dockalová (Moravské Zemské Muzeum, Anthropos Institute, Brno, Czech Republic), Chris Stringer and Rob Kruszynski (Natural History Museum of London, England; National Museum of Wales, Cardiff), and Yoel Rak (Department of Anatomy and Anthropology, University of Tel Aviv, Israel). We wish also to thank Bence Viola for the casts of Sunghir. We are grateful to the "Neanderthal Studies Professional Online Service" (NESPOS Database/www.nespos.org), and convey our special thanks to Priscilla Bayle for her precious advice in downloading 3D models from the NESPOS internet platform. Many thanks to Dick Byer for proofreading this manuscript. We thank A. G. Drake for his help with the English language on the final version of the manuscript.

LITERATURE CITED

Bailey SE. 2002. A closer look at Neanderthal postcanine dental morphology: the mandibular dentition. Anat Rec 269:148–156.

Bailey SE. 2004. A morphometric analysis of maxillary molar crowns of Middle-Late Pleistocene hominins. J Hum Evol 47:183–198.

Bailey SE, Hublin JJ. 2006. Dental remains from the Grotte du Renne at Arcy-sur-Cure (Yonne). J Hum Evol 50:485–508.

Bailey SE, Lynch JM. 2005. Diagnostic differences in mandibular P4 shape between Neanderthals and anatomically modern humans. Am J Phys Anthropol 126:268–277.

Bailey SE, Pilbrow VC, Wood BA. 2005. Interobserver error involved in independent attempts to measure cusp base areas of PanM1s. J Anat 205:323–331.

Benazzi S, Fantini M, De Crescenzio F, Persiani F, Gruppioni G. 2009. Improving the spatial orientation of human teeth using a virtual 3D approach. J Hum Evol 56:286–293.

Beraldin JA, Blais F, Cournoyer L, Godin G, Rioux M. 2000. Active 3D sensing. Modelli e metodi per lo studio e la conservazione dell'architettura storica, Scuola Normale Superiore Pisa. Quaderni 10:22–46.

Biggerstaff RH. 1970. A quantitative and qualitative study of the post-canine dentition of twins. Ann Arbor: University Microfilms.

Breuckmann B. 1993. Bildverarbeitung und optische Meßtechnik in der industriellen Praxis. München: Franzis.

Coppa A, Grün R, Stringer C, Eggins S, Vargiu R. 2005. Newly recognized Pleistocene human teeth from Tabun Cave, Israel. J Hum Evol 49:301–315.

Erdbrink DP. 1965. A quantification of the Dryopithecus and other lower molar patterns in man and some of the apes. Z Morphol Anthropol 57:70–108.

Fiorenza L, Benazzi S, Kullmer O. 2009. Morphology, wear and 3D digital surface models: materials and techniques to create high-resolution replicas of teeth. J Anthropol Sci 87:211–218.

Godin G, Beraldin JA, Taylor J. 2002. Active optical 3D imaging for heritage applications. IEEE CG&A 22:24–36.

Gómez-Robles A, Martinón-Torres M, Bermúdez de Castro JM. 2007. A geometric morphometric analysis of hominin upper first molar shape. J Hum Evol 53:272–285.

Goose DH. 1963. Dental measurement: an assessment of its value in anthropological studies. In: Brothwell DR, editor. Dental anthropology. London: Pergamon Press. p 125–148.

Hanihara K. 1961. Criteria for classification of crown characters of the human deciduous dentition. J Anthropol Soc Nippon 69:27–45.

Hanihara K, Tamada M, Tanaka T. 1970. Quantitative analysis of the hypocone in the human upper molars. J Anthropol Soc Nippon 78:200–207.

Harris EF, Dinh DP. 2006. Intercusp relationships of the permanent maxillary first and second molars in American whites. Am J Phys Anthropol 130:514–528.

Harris EF, Lease LR. 2005. Mesiodistal tooth crown dimensions of the primary dentition: a worldwide survey. Am J Phys Anthropol 128:593–607.

Hillson S, Fitzgerald C, Flinn H. 2005. Alternative dental measurements: proposals and relationships with other measurements. Am J Phys Anthropol 126:413–426.

Işcan MY, Kedici PS. 2003. Sexual variation in bucco-lingual dimensions in Turkish dentition. Forensic Sci Int 137:160–164.

Kaifu Y, Arif J, Yokoyama K, Baba H, Suparka E, Gunawan H. 2007. A new *Homo erectus* molar from Sangiran. J Hum Evol 52:222–226.

Kieser JA. 1990. Human adult odontometrics. Cambridge: Cambridge University Press.

Kondo S, Townsend GC. 2006. Associations between Carabelli trait and cusp areas in human permanent maxillary first molars. Am J Phys Anthropol 129:196–203.

Kullmer O, Huck M, Engel K, Schrenk F, Bromage TG. 2002. Hominid Tooth Pattern Database (HOTPAD) based on optical 3D topometry. In: Mafart B, Delingette H, editors. Three-dimensional imaging in paleoanthropology and prehistoric archaeology, Acts of the XIVth UISPP Congress, University of Liège, Belgium, 2–8 September 2001, Colloque, Symposium 1.7 BAR International Series 1049. p 71–82.

Le Blanc SA, Black B. 1974. A long term trend in tooth size in the eastern Mediterranean. Am J Phys Anthropol 41:417–422.

Martinón-Torres M, Bastir M, Bermúdez de Castro JM, Gómez A, Sarmiento S, Muela A, Arsuaga JL. 2006. Hominin lower second premolar morphology: evolutionary inferences through geometric morphometric analysis. J Hum Evol 50:523–533.

Matsumura H, Hudson MJ. 2005. Dental perspectives on the population history of Southeast Asia. Am J Phys Anthropol 127:182–209.

Moorrees CFA, Reed RB. 1954. Correlations among crown diameters of human teeth. Arch Oral Biol 9:685–697.

Morris DH. 1986. Maxillary molar occlusal polygons in five human samples. Am J Phys Anthropol 70:333–338.

Peretz B, Nevis N, Smith P. 1997. Morphometric variables of developing primary maxillary first molar crowns in humans. Arch Oral Biol 42:423–427.

Peretz B, Nevis N, Smith P. 1998a. Morphometric analysis of developing crowns of maxillary primary second molars and permanent first molars in humans. Arch Oral Biol 43:525–533.

Peretz B, Shapira J, Farbstein H, Arieli E, Smith P. 1998b. Modified cuspal relationships of mandibular molar teeth in children with Down's syndrome. J Anat 193:529–533.

Peretz SI, Bernal V, Gonzalez PN. 2006. Differences between sliding semi-landmark methods in geometric morphometrics, with an application to human craniofacial and dental variation. J Anat 208:769–784.

Pilbrow V. 2006. Population systematics of chimpanzees using molar morphometrics. J Hum Evol 51:646–662.

R Development Core Team. 2008. R: a language and environment for statistical computing. Vienna, Austria: R Foundation for Statistical Computing.http://www.r-project.org.

Sekikawa M, Kanazawa E, Ozaki T, Brown T. 1988. Principal component analysis of intercusp distances on the lower first molars of three human populations. Arch Oral Biol 33:535–541.

Smith BH. 1984. Patterns of molar wear in hunter-gatherers and agriculturalists. Am J Phys Anthropol 63:39–56.

Ulhaas L, Kullmer O, Schrenk F, Henke W. 2004. A new 3-d approach to determine functional morphology of cercopithecoid molars. Ann Anat 186:487–494.

Williams LR. 1979. A photogrammetrical analysis of the pongid molar morphology. PhD dissertation, University of Toronto.

Wood BA. 1991. Koobi Fora Research Project, Vol. 4: Hominid cranial remains. Oxford: Clarendon Press.

Wood BA, Abbott SA. 1983. Analysis of the dental morphology of Plio-Pleistocene hominids. I. Mandibular molars: crown area measurements and morphological traits. J Anat 136: 197–219.

Wood BA, Abbott SA, Graham SH. 1983. Analysis of the dental morphology of Plio-Pleistocene hominids. II. Mandibular molars-study of cusp areas, fissure pattern and cross sectional shape of the crown. J Anat 137:287–314.

Wood BA, Engleman CA. 1988. Analysis of the dental morphology of Plio-Pleistocene hominids. V. Maxillary postcanine tooth morphology. J Anat 161:1–35.